

GLYCEROL-INTERCALATED Mg-Al HYDROTALCITE AS A POTENTIAL SOLID BASE CATALYST FOR TRANSESTERIFICATION

YUANZHOU XI AND ROBERT J. DAVIS*

Department of Chemical Engineering, University of Virginia, 102 Engineers' Way, PO Box 400741, Charlottesville, VA 22904-4741, USA

Abstract—Glycerol is a byproduct of biodiesel synthesis by transesterification of triglycerides with short-chain alcohols in the presence of solid base catalysts. Because hydrotalcite is a potentially useful basic catalyst for the transesterification reaction, the interaction of glycerol with hydrotalcite is the focus of this work. Glycerol was intercalated into Mg-Al hydrotalcite with a Mg/Al molar ratio of 4 under elevated temperatures of 443–503 K in the absence and presence of NaOH. The resulting materials were characterized by X-ray diffraction, Fourier transform infrared spectroscopy, thermogravimetric analysis, and N₂ adsorption. The amount of glycerol incorporated into hydrotalcite increased with increasing temperature of intercalation. However, the brucite-like sheets of hydrotalcite partially decomposed during the intercalation process at the highest temperature. The presence of NaOH stabilized the hydrotalcite layers against decomposition under high temperature (503 K). The intercalated materials exposed large surface areas ranging from 142 to 663 m² g⁻¹, depending on the preparation conditions. The glycerol-intercalated hydrotalcites were less catalytically active than hydrotalcite with OH⁻ counterions for the transesterification of tributyrin with methanol. The lower reactivity of glycerol-intercalated hydrotalcite was probably the result of a strong interaction between the intercalated glycerolate (HOCH₂-CHOH-CH₂O⁻) and the partially decomposed brucite-like sheets.

Key Words—Biodiesel, Catalyst, DTG, FTIR, Glycerol, Hydrotalcite, TGA, Transesterification, Tributyrin, XRD.

INTRODUCTION

Magnesium aluminum hydroxycarbonate (Mg-Al hydrotalcite) with a general chemical composition of [Mg_(1-x)Al_x³⁺(OH)₂]^{x+}CO₃^{2-x/2}·nH₂O is a widely studied anionic clay material because of its potential applications as an adsorbent, catalyst, ion-exchange medium, and drug-delivery vehicle (Cavani *et al.*, 1991; Sels *et al.*, 2001; Williams and O'Hare, 2006; Debecker *et al.*, 2009). The crystal structure of hydrotalcite is related to the layered material brucite in which Mg cations are octahedrally coordinated to hydroxyl groups. Hydrotalcite materials have brucite-like sheets in which some of the Mg cations are replaced by Al cations, thus creating a positive charge on the layers which is balanced by common interlayer anions such as carbonate, sulfate, halide, nitrate, and hydroxyl. Water molecules are generally present with the interlayer anions.

Thermal decomposition of Mg-Al hydrotalcite with carbonate anions generates a Mg-Al mixed oxide with large surface area and exposed base sites that can function as catalysts for a variety of reactions, such as alcohol dehydrogenation and/or dehydration (McKenzie *et al.*, 1992; Fishel and Davis, 1994a, 1994b; Di Cosimo

et al., 1998), aldol condensation (Reichle, 1985), and double-bond isomerization (Beres *et al.*, 1999). The properties of the hydrotalcite-derived base sites depend mainly on the Mg/Al ratio and the preparation method of the hydrotalcite precursor (Cavani *et al.*, 1991; McKenzie *et al.*, 1992; Fishel and Davis, 1994a, 1994b; Di Cosimo *et al.*, 1998). Rehydration of a Mg-Al mixed oxide derived from hydrotalcite can reform the brucite-like layered structure of hydrotalcite with hydroxyl groups serving as charge-balancing anions instead of carbonate. The interlayer OH⁻ anions are Brønsted bases with excellent catalytic function in base-catalyzed reactions such as aldol condensation (Rao *et al.*, 1998; Tichit *et al.*, 1998; Winter *et al.*, 2006), Michael addition (Choudary *et al.*, 1999), and transesterification of tributyrin with methanol (Cantrell *et al.*, 2005; Xi and Davis, 2008, 2009).

Choudary *et al.* (2000, 2003) reported recently that tert-butoxide Mg-Al hydrotalcite exhibited greater reactivity than OH⁻-containing hydrotalcite for transesterification and the Wadsworth–Emmons reaction. Moreover, Gardner *et al.* (2001) showed that alkoxide-intercalated hydrotalcite-like materials can expose very large surface areas of 400–600 m² g⁻¹. Intercalation compounds with alkoxides as charge-balancing anions are, therefore, potentially useful materials for applications requiring basic sites and/or larger surface areas. Thus, polyols such as ethylene glycol or glycerol have been intercalated into brucite (Wypych *et al.*, 2002), ZnAlCO₃ layered double hydroxide (Guimaraes *et al.*,

* E-mail address of corresponding author:

rjd4f@virginia.edu

DOI: 10.1346/CCMN.2010.0580403

2000), Mg-Al hydrotalcite (Hansen and Taylor, 1991; Stanimirova and Hibino, 2006), and layered yttrium hydroxide (Xi and Davis, 2010).

In this work, glycerol was intercalated into Mg-Al hydrotalcite with a Mg/Al molar ratio of 4 under elevated temperature from 443 K to 503 K in the presence and absence of NaOH. Glycerol was selected as the target polyol because it is the final side product of base-catalyzed transesterification of triglycerides with short-chain alcohols to produce biodiesel. If hydrotalcite catalysts for biodiesel synthesis are to be developed for commercial use, the intercalation chemistry of glycerol and the reactivity of the resulting inorganic-organic composite need to be evaluated. The reactivity of the glycerol-intercalated hydrotalcite was evaluated and compared to that of a reconstructed hydrotalcite in the OH⁻ form for the transesterification of tributyrin with methanol as a model reaction for biodiesel synthesis.

EXPERIMENTAL METHODS

Material synthesis

A constant pH coprecipitation method was used to prepare Mg-Al hydrotalcite with a Mg/Al molar ratio of 4. A 300 mL aqueous solution containing 92.28 g (0.36 mol) of Mg(NO₃)₂·6H₂O (Acros, 98%) and 33.75 g (0.09 mol) of Al(NO₃)₃·9H₂O (Aldrich, 98%) and another 300 mL aqueous solution containing 9.54 g (0.09 mol) of Na₂CO₃ (Aldrich, 99.95%) were added dropwise to 80 mL of distilled deionized (DDI) water that was stirred vigorously at 333 K over ~30 min. The pH of the mixture was maintained at 10 by adding dropwise a 4.0 mol L⁻¹ solution of NaOH (Mallinckrodt, 99%). After the slurry was stirred for 24 h at 333 K, the white precipitate was recovered by centrifugation and washed thoroughly with hot (~333 K) DDI water. The precipitate was then oven dried in air at 338 K for 24 h, ground into a powder, and sieved between 0.038 mm and 0.075 mm. The resulting material is denoted as HT.

The OH⁻ form of Mg-Al hydrotalcite was prepared by thermal decomposition followed by reconstruction in liquid water. The decomposed Mg-Al hydrotalcite was prepared by heating 0.5 g of HT sample under flowing dry N₂ (100 cm³ min⁻¹) (Messer, 99.999%) at 723 K (after heating at a rate of 10 K min⁻¹) for 8 h. The decomposed hydrotalcite was reconstructed by dispersing the decomposed 0.5 g of Mg-Al hydrotalcite into 50 mL of decarbonated DDI water and stirring at 800 rpm for 5 h at room temperature under flowing N₂ (40 cm³ min⁻¹). The solid material, denoted as HT-R, was separated by centrifugation and washed with 200 mL of anhydrous methanol (Sigma-Aldrich, 99.8%).

The intercalation of glycerol into hydrotalcite was accomplished by the following procedure: 1.0 g of NaOH (Mallinckrodt, 99%) was dissolved in 50 mL of glycerol (99.6%, Acros) at ~373 K, under magnetic stirring at 800 rpm. The freshly prepared HT-R from

0.5 g of HT was then added to the NaOH/glycerol solution and the mixture was stirred at 800 rpm at a selected temperature (443, 453, 463, 483, or 503 K) for 2 h under flowing N₂ (100 cm³ min⁻¹). The mixture was then cooled to room temperature and diluted with 50 mL of methanol. The product was separated by centrifugation and washed with an additional 350 mL of methanol. Finally, the material was dried under flowing N₂ (100 cm³ min⁻¹, Messer, 99.999%) overnight at room temperature. The materials obtained were denoted as HT-R-NaGL-TTT, where TTT indicates the treatment temperature in Kelvin.

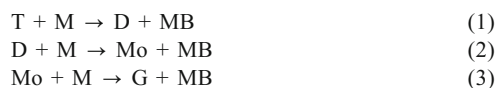
The intercalation of glycerol into reconstructed hydrotalcites was also performed as described above at 443 K and 503 K but without adding any NaOH to the solutions. The samples prepared without NaOH were denoted as HT-R-GL-443 and HT-R-GL-503.

Characterization of material

Thermogravimetric analysis (TGA) was performed using a TGA 2050 Thermogravimetric Analyzer (TA Instruments, New Castle, Delaware, USA). Approximately 40 mg of solid sample was loaded into the instrument and the temperature was ramped from room temperature to 1073 K at 2 K min⁻¹ under 100 cm³ min⁻¹ of flowing air. X-ray diffraction (XRD) was obtained using a Scintag XDS 2000 diffractometer using CuK α radiation ($\lambda = 1.54 \text{ \AA}$). Fourier transform infrared (FTIR) spectra were recorded using a BIO-RAD FTS-60A spectrometer equipped with a liquid N₂-cooled MCT detector (Bio-Rad Laboratories Inc., Cambridge, Massachusetts, USA). Solid samples were diluted in KBr powder at 5 wt.% and spectra were measured in the diffuse reflectance mode using a Harrick Praying Mantis diffuse reflectance accessory (Harrick Scientific Products, Inc., Pleasantville, New York). A liquid glycerol sample was examined in the transmission mode. All spectra were averaged by accumulating 100 scans at a resolution of 4 cm⁻¹ over the range 4000–400 cm⁻¹. The N₂-adsorption experiments were performed using a Micromeritics ASAP 2020 adsorption system (Micromeritics Instrument Corporation, Norcross, Georgia, USA) operated at 77 K. The surface areas and pore-size distributions of the solid samples were calculated based on the Brunauer-Emmett-Teller (BET) method and Barrett-Joyner-Hallender (BJH) method, respectively.

Transesterification

Transesterification of tributyrin with methanol was used as a probe reaction for the intercalated samples. The transesterification of tributyrin (T) with methanol (M) proceeds in three consecutive steps as shown below with methyl butyrate (MB) and glycerol (G) as final products and dibutyryl (D) and monobutyryl (Mo) as intermediate products (Cantrell *et al.*, 2005; Xi and Davis, 2008, 2009).



The reaction was performed in a 250 mL 3-neck round-bottom flask maintained at 333 K by a heated oil bath and equipped with a magnetic stirrer operated at 800 rpm. The reactor was purged continuously with flowing N_2 at $40 \text{ cm}^3 \text{ min}^{-1}$ which vented through a reflux condenser. In each run, 68.25 g of methanol and 21.9 g of purified tributyrin (Xi and Davis, 2009) were charged into the reactor with 3.3 g of dibutyl ether (Aldrich, 99.3%) as an internal standard. After the temperature of the reactants reached 333 K, the freshly prepared intercalated hydrotalcite was added directly to the reactor to initiate transesterification. Liquid samples were removed from the reactor at different time intervals and analyzed for products using the same procedure described in previous studies (Xi and Davis, 2008, 2009). The recyclability of one catalyst (HT-R-GL-443) was tested by separating the solid from the liquid products by centrifugation after 15 h of reaction and charging it back into the reactor with fresh reactants. After the second reaction was run for a further 15 h, the catalyst was again removed by centrifugation, washed with 200 mL of methanol, and dried under flowing N_2 ($100 \text{ cm}^3 \text{ min}^{-1}$) at room temperature prior to characterization by XRD and FTIR spectroscopy.

RESULTS

X-ray diffraction

X-ray diffraction was used to characterize the crystal structure of HT and its derived materials (Figure 1). The parent HT sample and its OH^- analog HT-R exhibit typical reflections from the regular layers at $\sim 11.1^\circ 2\theta$ and $22.4^\circ 2\theta$, corresponding to 003 and 006 reflections of hydrotalcite-type materials. The interlayer distances of

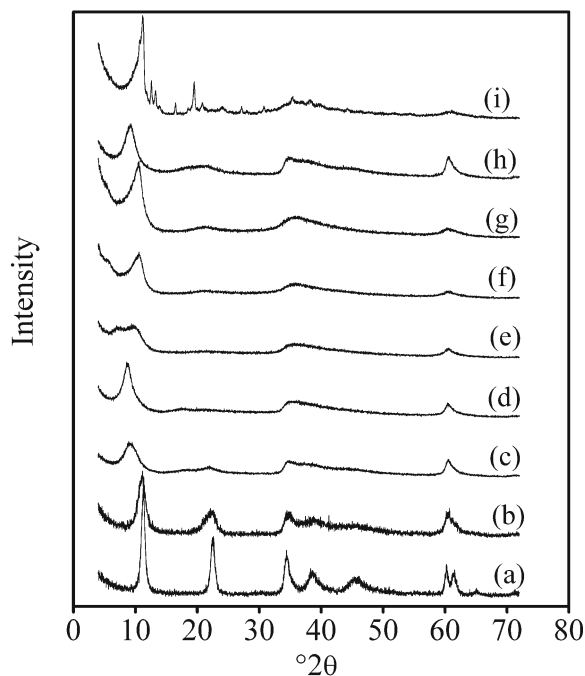


Figure 1. XRD patterns of (a) HT; (b) HT-R; (c) HT-R-NaGL-443; (d) HT-R-NaGL-453; (e) HT-R-NaGL-463; (f) HT-R-NaGL-483; (g) HT-R-NaGL-503; (h) HT-R-GL-443; and (i) HT-R-GL-503.

HT and its derived materials were calculated based on the position of the 003 reflection (Table 1). The features associated with 110 appeared at $\sim 60.3^\circ 2\theta$ and are related to the octahedral units of the brucite-like sheet. The HT-R sample had a slightly expanded interlayer distance of 8.02 Å compared to that of HT which was 7.86 Å. The 003 peak of HT-R was broader than that of HT, however, suggesting a smaller crystal size or greater disorder in the HT-R samples (Xi and Davis, 2009). After intercalation of glycerol in the presence of NaOH at

Table 1. Physical properties of HT and its derived materials.

Sample	Interlayer distance ^a (Å)	S_{BET} ($\text{m}^2 \text{ g}^{-1}$)	Mass loss 296–400 K (wt.%)	Mass loss 400–1073 K (wt.%)
HT	7.86	54	16.17 ^b	29.96 ^c
HT-R	8.02	69	19.00 ^b	25.28 ^c
HT-R-NaGL-443	9.54	178	8.03	44.30
HT-R-NaGL-453	10.12	218	8.93	47.58
HT-R-NaGL-463	12.11, 8.90 ^d	291	8.80	49.93
HT-R-NaGL-483	7.98	509	8.28	51.19
HT-R-NaGL-503	8.08	663	5.31	52.47
HT-R-GL-443	9.66	142	8.16	44.95
HT-R-GL-503	7.76	431	4.65	54.74

^a Calculated from the 003 reflection of the XRD results

^b Mass loss in the temperature range 296–473 K

^c Mass loss in the temperature range 473–1073 K

^d Based on the two separate 003 reflections

temperatures from 443 K to 503 K, the 003 reflection broadened further and shifted to lower angles (Figure 1). The expansion of the interlayer distance is consistent with glycerol intercalation in the presence of NaOH. However, as the temperature of the intercalation increased from 453 K to 483 K or 503 K, the interlayer distance contracted to a value similar to the parent HT and HT-R. HT-R-NaGL-463 revealed two overlapping (003) reflections at $\sim 7.3^\circ 2\theta$ and $\sim 9.9^\circ 2\theta$ (Figure 1). The 110 reflections of glycerol-intercalated samples prepared in the presence of NaOH remained constant at $\sim 60.3^\circ 2\theta$, although the peak intensity decreased with increasing temperature of intercalation. When the glycerol was intercalated without the presence of NaOH, the XRD pattern of the sample prepared at 443 K was quite similar to that prepared with NaOH (Figure 1). However, increasing the intercalation temperature to 503 K caused new features to appear (Figure 1i). The 110 reflection of HT-R-GL-503 was barely discernible and the feature at $11.4^\circ 2\theta$, assumed to be associated with the 003 reflection of a layered material, indicates a significant

contraction of the layer spacing. Evidently, intercalation of glycerol into HT-R at 503 K without the presence of NaOH could lead to the formation of crystal phases other than the layered structure.

Fourier transform infrared spectroscopy

FTIR spectroscopy was also used to characterize HT and its derived materials (Figure 2). The HT sample exhibited a broad band at $\sim 3590\text{ cm}^{-1}$, which is ascribed to the stretch of the hydroxyl groups of the brucite-like sheets (Kloprogge and Frost, 1999; Xi and Davis, 2009). The broad shoulder at $\sim 3000\text{ cm}^{-1}$ is attributed to the H-bonding between the crystalline water and carbonate anion (Kloprogge and Frost, 1999; Xi and Davis, 2009). The asymmetric stretching of the carbonate anion has a strong absorption band at 1370 cm^{-1} . The band at $\sim 1642\text{ cm}^{-1}$ can be ascribed to the bending mode of molecular water. The spectrum of decomposed and reconstructed HT-R was similar to that of HT because thermal treatment at 723 K is inadequate to remove all of the carbonate associated with HT (Xi and Davis, 2009).

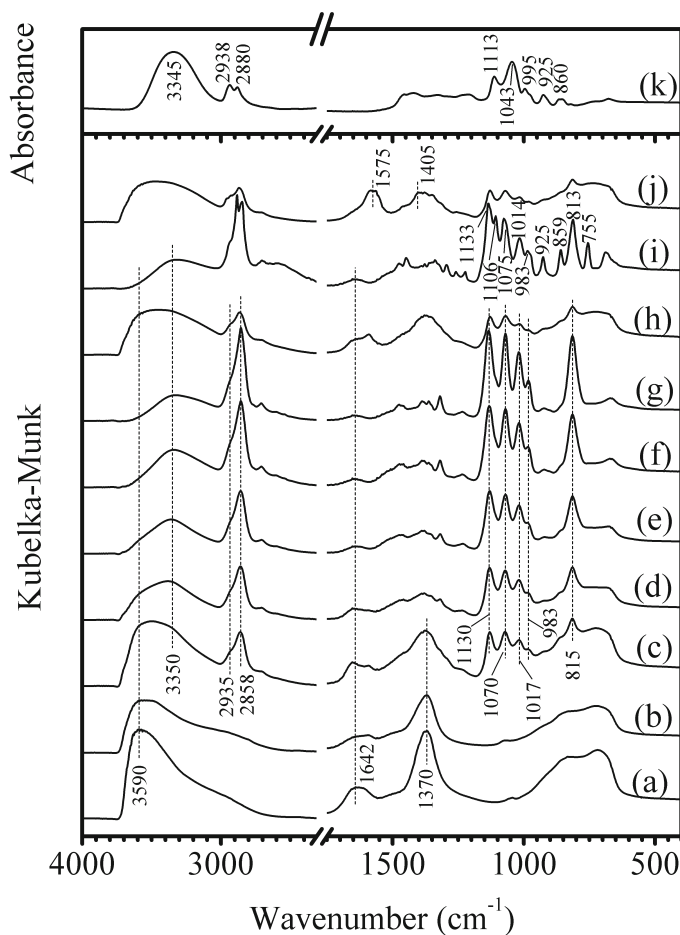


Figure 2. FTIR spectra of (a) HT; (b) HT-R; (c) HT-R-NaGL-443; (d) HT-R-NaGL-453; (e) HT-R-NaGL-463; (f) HT-R-NaGL-483; (g) HT-R-NaGL-503; (h) HT-R-GL-443; (i) HT-R-GL-503; (j) HT-R-GL-443 after two transesterification reaction cycles; and (k) liquid glycerol.

The asymmetric stretching of carbonate at 1370 cm^{-1} of HT-R was still present in the spectrum of HT-R (Figure 2b). The appearance of C–H bands at 2858 cm^{-1} and 2935 cm^{-1} in the IR spectra (Figure 2c–g) of HT-R after intercalation of glycerol at temperatures from 443 K to 503 K in the presence of NaOH was consistent with intercalation of glycerol into the interlayer spaces of hydrotalcite as suggested by XRD. The C–H bands were shifted slightly from those of liquid glycerol (Figure 2k) at 2880 cm^{-1} and 2938 cm^{-1} (Mendelovici *et al.*, 2000). The four bands at 1130 , 1070 , 1017 , and 983 cm^{-1} , observed on the glycerol-intercalated samples prepared with NaOH, were probably associated with glycerol absorption bands at 1113 , 1043 , and 995 cm^{-1} (Mendelovici *et al.*, 2000). The band at 815 cm^{-1} might be attributed to the C–C stretching band of glycerol appearing at 860 cm^{-1} in the liquid.

The narrowing of the bands of glycerol-intercalated HT-R with NaOH in the range $800\text{--}1200\text{ cm}^{-1}$ is thought to be a consequence of localizing the molecules in a crystalline solid. A similar effect was reported on a zinc glycerolate material (Remias *et al.*, 2009). The relative intensity of the peaks associated with glycerol in the range $800\text{--}1200\text{ cm}^{-1}$ increased as the treatment temperature increased from 443 K to 503 K for samples prepared with NaOH. On the other hand, the intensity of the hydroxyl stretch associated with the hydroxyl layers at 3590 cm^{-1} decreased significantly as the treatment temperature increased, especially above 463 K. The hydroxyl groups of hydrotalcite, especially those bonded to Al, begin to decompose at $\sim 473\text{ K}$. Bellotto *et al.* (1996) used ^{27}Al MAS-NMR spectroscopy to observe the transformation of Al atoms at 473 K in octahedral sites of Mg-Al hydrotalcite to tetrahedral sites. The dehydroxylation of Mg-Al hydrotalcite was observed by XAFS to begin in the range $425\text{--}473\text{ K}$, as reported by van Bokhoven *et al.* (2001). Yang *et al.* (2002) used diffuse reflectance infrared Fourier transform spectra (DRIFTS) to determine that the hydroxyl groups bonded to Al cations of Mg-Al hydrotalcite started to decompose at 463 K. Moreover, Rey and Fornes (1992) found that the intensity of IR and ^1H nuclear magnetic resonance (NMR) signals associated with the hydroxyl groups of hydrotalcite layers decreased in intensity in the range $373\text{--}500\text{ K}$. By comparing the relative absorption intensity between the hydroxyl stretch of glycerol at $\sim 3345\text{ cm}^{-1}$ and the C–H stretch of glycerol at 2938 and 2880 cm^{-1} (Figure 2k), a clear modification of glycerol in the intercalated hydrotalcites was observed (Figure 2c–g). The change in the relative intensity of the IR bands can be attributed to a decrease in the H-bonding between the hydroxyl groups of the intercalated glycerol moiety (Zelent *et al.*, 2004; Dashnau *et al.*, 2006). The feature for the bending mode of water at $\sim 1642\text{ cm}^{-1}$ of the samples intercalated with glycerol in the presence of NaOH decreased in intensity as the

treatment temperature increased from 443 K to 503 K, which is consistent with water being removed from the interlayer regions at elevated temperature. The similarity of the IR spectra of HT-R-GL-443 (Figure 2h) and HT-R-NaGL-443 (Figure 2c) indicate very little role for NaOH in the intercalation at 443 K. However, the significant differences between samples prepared at 503 K (Figure 2i and 2g) illustrated the significant role of NaOH at the elevated temperature. Indeed, new crystalline phases were detected by XRD for a sample prepared at 503 K in the absence of NaOH (Figure 1i).

Thermogravimetric analysis

The thermal stability of HT and its derived materials was evaluated by thermogravimetric analysis (TGA) and differential thermogravimetric analysis (DTG) (Figure 3). The HT and HT-R samples exhibited the typical two-step mass-loss process during thermal decomposition. For example, HT and HT-R experienced 16.17% and 19.00% mass loss, respectively, below

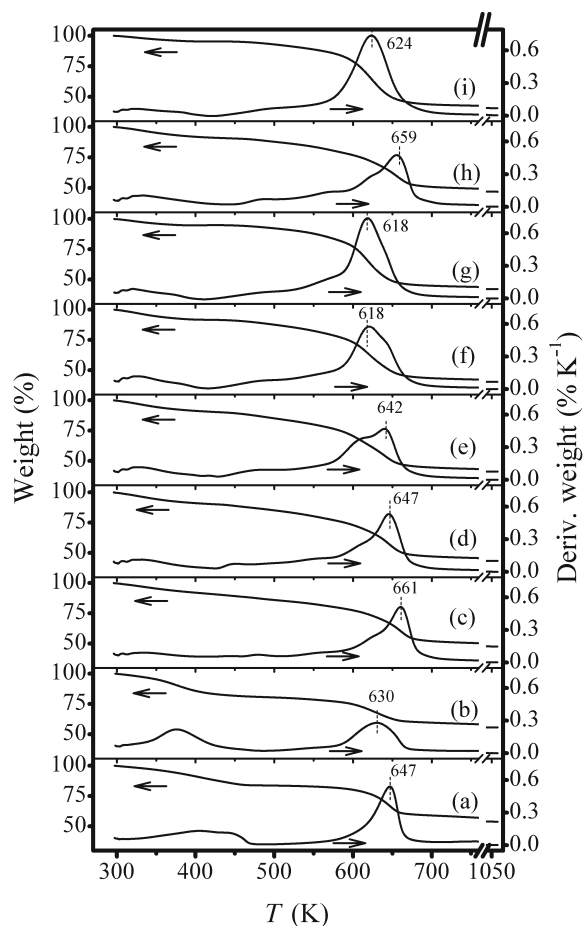


Figure 3. TGA and DTG analyses of (a) HT; (b) HT-R; (c) HT-R-NaGL-443; (d) HT-R-NaGL-453; (e) HT-R-NaGL-463; (f) HT-R-NaGL-483; (g) HT-R-NaGL-503; (h) HT-R-GL-443; and (i) HT-R-GL-503.

473 K, which is due to the removal of molecular water (Tichit *et al.*, 1995, 1998). The mass losses from HT and HT-R above 473 K (Table 1) are ascribed to the simultaneous decomposition of the brucite-like sheets and the interlayer anions (CO_3^{2-} for HT and OH^- for HT-R). The HT sample was slightly more stable than HT-R as the DTG peak for decomposition was at 647 K compared to 630 K in the latter (Figure 3).

According to the TGA and DTG results (Figure 3), all the materials with glycerol had 4–9% mass loss below 400 K, which is probably due to the loss of adsorbed solvent methanol, and a major mass loss in the range 600–670 K, which can be ascribed to the decomposition of the layered hydroxide and vaporization/oxidation of glycerol. The mass losses between 400–1073 K of hydrotalcite intercalated with glycerol (Table 1) were significantly greater than that of either HT or HT-R, confirming again the incorporation of glycerol into HT-R. The mass loss above 400 K for intercalated samples with NaOH increased from 44.30% to 52.47% as the treatment temperature increased from 443 K to 503 K, indicating a greater loading of glycerol at higher temperatures.

N_2 adsorption

The N_2 adsorption-desorption isotherms of HT-R and its glycerol intercalated analogs (Figures 4, 5) were used to characterize the textural properties of the samples. The samples had a type II adsorption isotherm with hysteresis loop on the desorption branch. The BJH pore-size distributions (Figure 6) were calculated from the adsorption isotherms. The two samples treated at the highest two

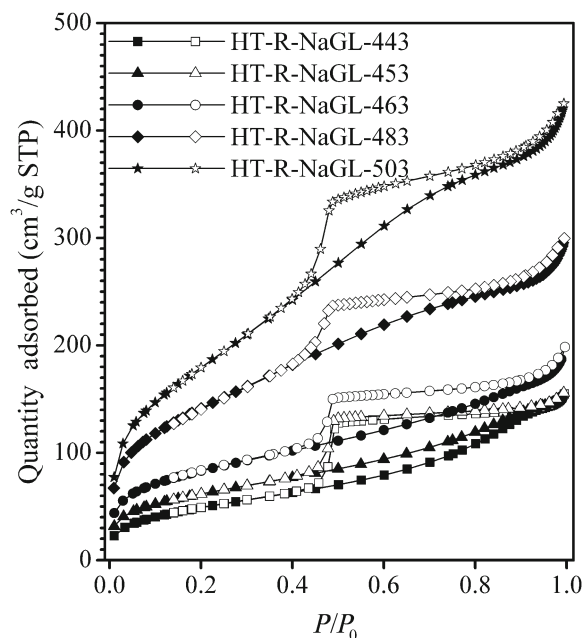


Figure 4. N_2 adsorption (solid symbols) and desorption (open symbols) isotherms of glycerol-intercalated HT-R prepared in the presence of NaOH at temperatures ranging from 443 to 503 K.

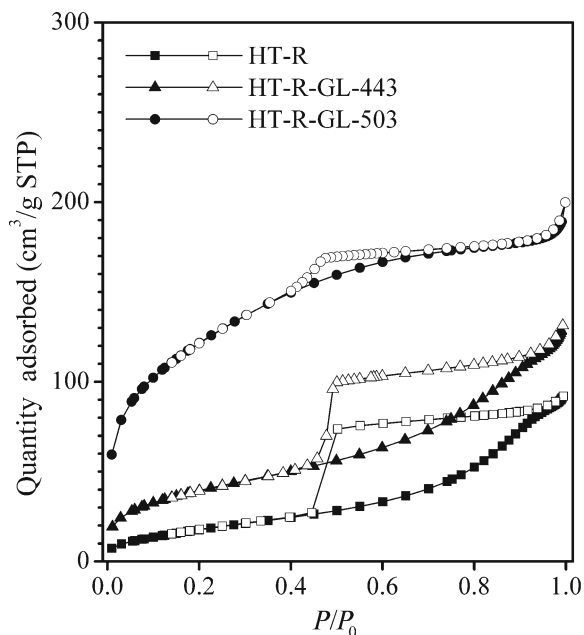


Figure 5. N_2 adsorption (solid symbols) and desorption (open symbols) isotherms of HT-R and glycerol-intercalated HT-R at 443 K and 503 K without NaOH.

temperatures with NaOH during glycerol intercalation, HT-R-NaGL-503 and HT-R-NaGL-483, had a maximum in the apparent pore-size distribution at ~ 3 nm. All of the other samples except for HT-R-GL-503, which is no

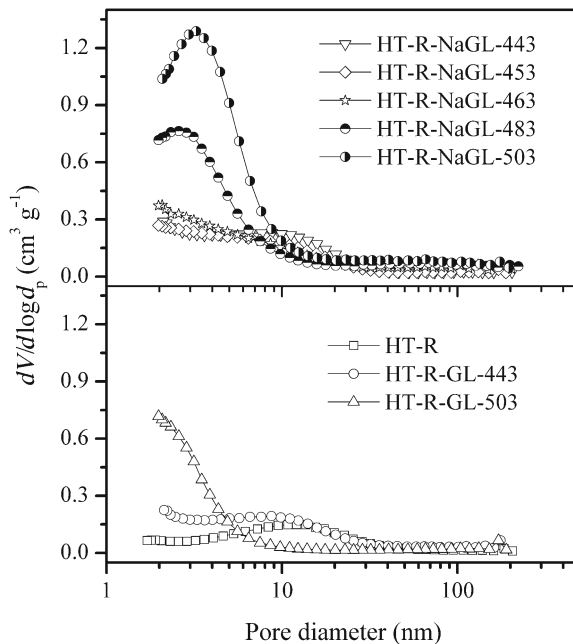


Figure 6. BJH pore-size distributions, derived from the N_2 adsorption branch of HT-R and its glycerol-intercalated analogs, with and without NaOH at temperatures of 443–503 K.

Table 2. Transesterification of tributyrin with methanol over hydrotalcite-derived catalysts.

Sample	Conversion of T ^a (%)	Yield of MB ^{a,f} (%)	Initial rate ($\mu\text{mol min}^{-1} \text{m}^{-2}$)	Initial rate ($\text{mmol min}^{-1} \text{g}^{-1}$)
HT-R ^c	98.3 ^b	96.1 ^b	40.4	2.79
HT-R-GL-443 ^d	92.8	89.2	6.65	0.94
HT-R-GL-443 ^{d,e}	82.2	69.0	3.81	0.54
HT-R-GL-503 ^d	53.0	23.9	0.40	0.17
HT-R-NaGL-443 ^d			12.1	2.15
HT-R-NaGL-503 ^d			1.94	1.29

^a At 800 min

^b At 200 min

^c Prepared from 1.0 g of HT

^d Prepared from 0.5 g of HT

^e Direct recycle experiment from HT-R-GL-433

^f Yield of MB: $y_{MB} = [MB]/[T]_0/3$, where $[MB]$ is the concentration of methyl butyrate (mol L^{-1}) and $[T]_0$ is the initial concentration of tributyrin (mol L^{-1}).

longer hydrotalcite, had a very broad pore-size distribution (Figure 6). The N_2 adsorption uptake increased significantly as the treatment temperature increased during glycerol intercalation into HT-R with NaOH (Figure 4). Indeed, the BET surface area increased monotonically as the treatment temperature increased (Table 1). The HT-R-NaGL-503 sample exposed a very large surface area of $663 \text{ m}^2 \text{ g}^{-1}$, which was much greater than its precursor HT and HT-R (Table 1). Gardner *et al.* (2001) also reported a series of alkoxide-intercalated hydrotalcite-like layered double hydroxides that had surface areas of $400\text{--}600 \text{ m}^2 \text{ g}^{-1}$. Intercalation of glycerol without NaOH also produced materials with large surface areas, but the resulting samples had smaller surface areas than those prepared with NaOH under the same temperature. Results from a t-plot (de Boer *et al.*, 1965) analysis (data not shown) indicated that the HT-R and its glycerol-intercalated analogs had negligible micropore surface area. The large surface area of glycerol-intercalated HT-R was, therefore, found in the broadly distributed mesopores.

Transesterification

The catalytic activities of reconstructed hydrotalcite and the glycerol-intercalated hydrotalcite catalysts for transesterification reaction were measured (Table 2). The reconstructed hydrotalcite with hydroxyl as the charge-balancing anion, HT-R, catalyzed the reaction at a faster rate than any of the glycerol-intercalated samples on both a catalyst-mass basis and a surface-area basis. At 200 min, HT-R prepared from 1.0 g of HT converted 98.3% of the tributyrin with a methyl butyrate yield of 96.1%. For HT-R-GL-443 prepared from 0.5 g of HT, 800 min were required to reach a tributyrin conversion of 92.8% with a methyl butyrate yield of 89.2%. Intercalated samples prepared with NaOH catalyzed transesterification with a greater specific rate than samples intercalated without NaOH (Table 2);

however, severe leaching of active species was detected on samples containing NaOH. The continued reaction of tributyrin in the reactant solution after removal of HT-R-NaGL-503 at 90 min was observed (Figure 7). The greater activity of HT-R-NaGL-443 and HT-R-NaGL-503 is, therefore, attributed to the residual sodium alkoxide or sodium hydroxide species that leached into the reaction medium.

The deactivation of reconstructed hydrotalcite (in the OH^- form) was observed in previous studies (Xi and Davis, 2008, 2009) and was mainly attributed to ester hydrolysis that produced butyrate anions. The butyrate anions subsequently replaced the hydroxyl anions in between the brucite-like sheets, thus deactivating the catalyst. The stability of glycerol-intercalated hydrotalcite

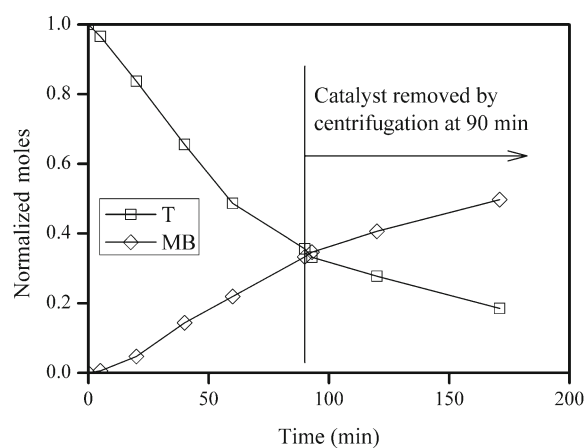


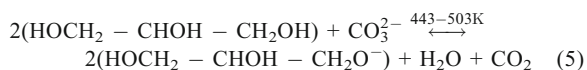
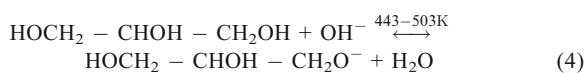
Figure 7. Reaction profile during transesterification of tributyrin with methanol over HT-R-NaGL-503. Catalyst was removed at 90 min. The normalized moles for T and MB are defined as $y_T = [T]/[T]_0$, $y_{MB} = [MB]/[T]_0/3$, respectively, where $[T]$ and $[MB]$ are the concentrations of tributyrin and methyl butyrate (mol L^{-1}), respectively, and $[T]_0$ is the initial concentration of tributyrin.

was investigated by recycling a sample that was prepared without NaOH. The initial rate of recycled HT-R-GL-443 was ~57.3% of its original level (Table 2). New absorption bands at ~1575 cm⁻¹ and ~1405 cm⁻¹, that appeared in the FTIR spectrum of HT-R-GL-443 after the second reaction (Figure 2j), are assigned to the asymmetric and symmetric stretching modes of carboxylate anions. This result is similar to previous findings on the deactivation of reconstructed hydrotalcites during transesterification (Xi and Davis, 2009). Evidently, some hydroxyl anions remained in the HT-R-GL-443 sample after glycerol intercalation and catalyzed the ester hydrolysis side reaction responsible for deactivation.

DISCUSSION

Characterization of samples by XRD, FTIR, and TGA confirmed that glycerol was successfully intercalated into hydrotalcite. The environment around the glycerol moieties was similar in all of the samples except HT-R-GL-503 because the FTIR spectra were largely independent of preparation conditions.

The intercalated glycerol was probably not the neutral molecule but rather glycerolate (HOCH₂-CHOH-CH₂O⁻) as suggested by Hansen and Taylor (1991). The glycerolate can be formed by the following reactions:



At the elevated temperatures of 443–503 K, the interlayer molecular water was eliminated and the reactions in equations 4 and 5 were likely to occur in the forward direction because CO₂ and H₂O were removed by the flowing N₂ (100 cm³ min⁻¹). The HT-R-NaGL-443 sample had an observable and broad carbonate absorption band at 1370 cm⁻¹ (Figure 2c). This carbonate band decreased significantly as the sample treatment temperature increased (Figures 2d–2g), suggesting that the reaction represented by equation 5 was favored at elevated temperature.

In the series of materials HT-R-NaGL-TTT (where TTT = 443, 453, 463, 483, and 503 K), the amount of intercalated glycerol as measured by TGA and FTIR spectroscopy appeared to increase with increasing temperature. However, the interlayer distance as evaluated by XRD increased after the lower-temperature intercalation procedure but decreased back to the original interlayer distance after higher-temperature treatments. The nature, amount, orientation, and stacking (monolayer or bilayer) of intercalated anions, as well as the presence of interlayer water, are known to affect the interlayer distance of intercalated hydrotalcite materials (Cavani *et al.*, 1991; Meyn *et al.*, 1990). For

example, Stanimirova and Hibino (2006) proposed that ethylene glycol intercalated into Mg-Al hydrotalcite had a bilayer of horizontally stacked ethylene glycol molecules between the adjacent hydrotalcite layers that had an interlayer distance of 13.7 Å. In the present study, the interlayer distances of glycerol intercalated HT-R samples in the presence of NaOH ranged from 7.98 to 12.11 Å (Table 1). Because the brucite-like sheet has a thickness of 4.8 Å (Perez-Ramirez *et al.*, 2007) and glycerol has a molecular diameter and length of 4.7 and 5.2 Å (Gordiyenko, *et al.*, 2004), respectively, the intercalated glycerol moieties in sample HT-R-NaGL-TTT should only have a monolayer arrangement within the interlayer space of brucite-like sheets. At the lower intercalation temperatures of 443 and 453 K, the intercalated glycerol appeared to be perpendicular to the layers as the interlayer spacing was greatest. At higher temperatures of 483 and 503 K, the interaction between the intercalated glycerol and layer became stronger due to the (partial) dehydroxylation of hydrotalcite, probably resulting in more horizontally arranged glycerol moieties between the layers with a much smaller interlayer distance of ~8 Å. The estimated interlayer space of HT-R-NaGL-483 and HT-R-NaGL-503 (3.2 Å) is much smaller than the glycerol molecule size, which is 4.7 Å in diameter and 5.2 Å long (Gordiyenko, *et al.*, 2004), strongly suggesting the penetration of glycerol moieties into the hydrotalcite layer. Wypych *et al.* (2002) proposed the formation of Mg–O–C bonds in ethylene glycol-intercalated brucite, based on an interlayer spacing that was significantly smaller than the molecule size of ethylene glycol. The interlayer space of the HT-R-NaGL-463 sample displayed two different interlayer separations of 12.11 and 8.90 Å. At ~463 K, the hydrotalcite layer probably began to experience significant dehydroxylation, resulting in the rearrangement of the intercalated glycerol moieties. The rearrangement led to an expanded interlayer distance of 12.11 Å as compared to that of HT-R-NaGL-443 or HT-R-NaGL-453.

The hydrotalcite structure of HT-R-GL-503 was largely destroyed and the XRD pattern (Figure 1i) and FTIR spectra (Figure 2i) of HT-R-GL-503 are significantly different from those of HT-R-NaGL-503 (Figures 1g, 2g). However, HT-R-GL-443 and HT-R-NaGL-443 have similar XRD patterns and FTIR spectra (Figures 1, 2). The presence of NaOH apparently prevented the decomposition of brucite-like sheets at 503 K. As discussed above, brucite-like sheets undergo (partial) dehydroxylation at or below ~473 K, with a greater extent of dehydroxylation occurring at the higher temperatures. The dehydroxylation probably occurs by reaction of hydroxyl groups in the same layer to release water (Rey and Fornes, 1992). The brucite-sheet dehydroxylation thus leads to the formation of crystal defects by exposing metal cations. However, the defects could be ‘healed’ by bonding to an available anion in the

region of the defect. The extent of healing-exposed cations probably depends on the concentration of the anion and its nature. During glycerol intercalation into HT-R at 503 K, with or without the presence of NaOH, the extent of hydrotalcite dehydroxylation is expected to be approximately the same as the temperature is identical. However, in the presence of NaOH, the concentration of glycerolate and OH^- in the medium will be much greater than without added NaOH. The exposed cations formed by dehydroxylation could, therefore, be coordinated to glycerolate and/or OH^- . The near absence of the hydroxyl group stretching vibration at $\sim 3590\text{ cm}^{-1}$ associated with the layers of HT-R-NaGL-503 (Figure 2g) indicates a replacement of layered hydroxyl groups by glycerolate. Equation 4 predicts that the equilibrium will favor the forward direction due to the greater amount of glycerol (0.68 mol) than sodium hydroxide (0.025 mol) and the continuous removal of H_2O as vapor at 503 K. Without the presence of NaOH, most of the defects (*i.e.* exposed cations) could not be healed by the glycerolate and/or OH^- . The new appearance of IR absorption bands at 1106, 925, 859, and 755 cm^{-1} (Figure 2i) probably indicates the presence of molecular glycerol on the exposed cations. On the other hand, when glycerol intercalation was performed at 443 K, the extent of dehydroxylation was much less than that at 503 K as indicated by significant hydroxyl vibrations at 3590 cm^{-1} associated with the layers of HT-R-GL-443 and HT-R-NaGL-443 (Figure 2c, 2h). The small amounts of cations exposed by dehydroxylation were, therefore, coordinated to glycerolate formed *in situ* as shown in equation 4.

The majority of the brucite-like sheets of HT and its glycerol-intercalated derivatives decomposed primarily between 600 K and 670 K (Figure 3). From the DTG curves of the glycerol-intercalated samples, the major mass loss occurred in the range 618–661 K, which is greater than the normal boiling point of glycerol (563 K). The glycerolate anions ($\text{HOCH}_2\text{-CHOH-CH}_2\text{O}^-$) in the interlayer regions of brucite-like sheets were probably released as neutral glycerol molecules during the decomposition process as the brucite-like sheets also decomposed in this temperature range. Proton transfer could readily occur between the hydroxyl groups of brucite-like sheets or product water molecules and the glycerolate. Wypych *et al.* (2002) studied the grafting of ethylene glycol and glycerol into brucite and the grafting of ethylene glycol into ZnAlCO_3 layered double hydr-oxide. In that work, they proposed the formation of covalent bonds between the polyol and the metal cations to give $M\text{-O-C}$, where M is Mg, Zn, or Al (Guimaraes *et al.*, 2000; Wypych *et al.*, 2002). Although no direct evidence was given for the formation of $M\text{-O-C}$ bonds in the present study, nor in the work of Guimaraes *et al.* (2000) or Wypych *et al.* (2002), the partial decomposition of the brucite-like sheets would

favor a direct interaction between the glycerolate anion ($\text{HOCH}_2\text{-CHOH-CH}_2\text{O}^-$) and the metal cations, thus replacing the missing OH^- groups.

The glycerol-intercalated hydrotalcite materials (HT-R-GL-443 and HT-R-GL-503) were less catalytically active for transesterification than HT-R, as presented above. The lesser activity of the glycerol-intercalated hydrotalcite can be explained by a strong interaction between the glycerolate and the partially decomposed brucite-like sheets. Moreover, the bulky glycerolate species in the hydrotalcite is probably less accessible in the interlayer regions than the highly mobile hydroxyl groups of the HT-R sample. Indeed, the reactivity of glycerol-intercalated hydrotalcite may be the result of residual hydroxyl in the sample. Butyrate anions were observed on HT-R-GL-443 after two transesterification runs *via* FTIR spectroscopy and hydroxyl anions catalyze the formation of the butyrate anion (Xi and Davis, 2009). These results contrast with those of Choudary *et al.* (2000, 2003) who reported that tert-butoxide Mg-Al hydrotalcite exhibited greater catalytic activity for base-catalyzed transesterification and the Wadsworth–Emmons reaction than the reconstructed hydrotalcite-containing hydroxyl counterions. In their case, however, interlayer water was not removed and the interlayer distance was not expanded after tert-butoxide intercalation. Thus, the intercalation was proposed to proceed inhomogeneously by a local distortion of the layers (Choudary *et al.*, 2003). Greenwell *et al.* (2003) performed a density functional theory study on the tert-butoxide Mg-Al hydrotalcite catalyzed transesterification. They reported that the active catalytic species on tert-butoxide Mg-Al hydrotalcite are the hydroxyl anions formed *in situ* through the hydrolysis of interlayer water with the tert-butoxide anions. In addition, the presence of interlayer water also facilitates the formation of reaction intermediates. Previous work by the present authors showed that removal of interlayer water in the reconstructed hydrotalcite increased the interaction between the hydroxyl anions and the brucite-like sheets and thus substantially reduced the catalytic activity for transesterification (Xi and Davis, 2008). Clearly, proper water management is critical for evaluation of hydrotalcite base catalysis for transesterification (Xi and Davis, 2009).

CONCLUSIONS

Glycerol was intercalated successfully into the reconstructed hydrotalcite under elevated temperature of 443–503 K, with or without the presence of NaOH. The amount of intercalated glycerol increased with treatment temperature. During the intercalation of glycerol, however, the brucite-like sheets decomposed partially and formed new crystalline phases. The presence of NaOH prevented complete decomposition of brucite-like sheets during the glycerol intercalation at

503 K. The BET surface area of glycerol-intercalated hydrotalcite increased monotonically with treatment temperature during the intercalation process. The glycerol-intercalated hydrotalcite was less active than an OH⁻-containing reconstructed hydrotalcite for the transesterification of tributyrin with methanol. The lesser activity of the glycerol-intercalated hydrotalcite was probably the result of a strong interaction between the glycerolate anion with the partially decomposed hydrotalcite layers.

ACKNOWLEDGMENTS

This work was supported by the Chemical Sciences, Geosciences and Biosciences Division, Office of Basic Energy Sciences, Office of Science, U.S. Department of Energy, grant No. DE-FG02-95ER14549.

REFERENCES

- Bellotto, M., Rebours, B., Clause, O., and Lynch, J. (1996) Hydrotalcite decomposition mechanism: A clue to the structure and reactivity of spinel-like mixed oxides. *Journal of Physical Chemistry*, **100**, 8535–8542.
- Beres, A., Palinko, I., Kiricsi, I., Nagy, J.B., Kiyozumi, Y., and Mizukami, F. (1999) Layered double hydroxides and their pillared derivatives – materials for solid base catalysis; synthesis and characterization. *Applied Catalysis a – General*, **182**, 237–247.
- Cantrell, D.G., Gillie, L.J., Lee, A.F., and Wilson, K. (2005) Structure-reactivity correlations in MgAl hydrotalcite catalysts for biodiesel synthesis. *Applied Catalysis a – General*, **287**, 183–190.
- Cavani, F., Trifiro, F., and Vaccari, A. (1991) Hydrotalcite-type anionic clays: preparation, properties and applications. *Catalysis Today*, **11**, 173–301.
- Choudary, B.M., Kantam, M.L., Reddy, C.R.V., Rao, K.K., and Figueras, F. (1999) The first example of Michael addition catalysed by modified Mg-Al hydrotalcite. *Journal of Molecular Catalysis a-Chemical*, **146**, 279–284.
- Choudary, B.M., Kantam, M.L., Reddy, C.V., Aranganathan, S., Santhi, P.L., and Figueras, F. (2000) Mg-Al-O-t-Bu hydrotalcite: a new and efficient heterogeneous catalyst for transesterification. *Journal of Molecular Catalysis a-Chemical*, **159**, 411–416.
- Choudary, B.M., Kantam, M.L., Reddy, C.R.V., Bharathi, B., and Figueras, F. (2003) Wadsworth-Emmons reaction: the unique catalytic reaction by a solid base. *Journal of Catalysis*, **218**, 191–200.
- Dashnau, J.L., Nucci, N.V., Sharp, N.K.A., and Vanderkooi, J.M. (2006) Hydrogen bonding and the cryoprotective properties of glycerol/water mixtures. *Journal of Physical Chemistry B*, **110**, 13670–13677.
- de Boer, J.H., Linsen, B.G., and Osinga, T.J. (1965) Pore systems in catalysts. VI. The universal t curve. *Journal of Catalysis*, **4**, 643–648.
- Debecker, D.P., Gaigneaux, E.M., and Busca, G. (2009) Exploring, tuning, and exploiting the basicity of hydrotalcites for applications in heterogeneous catalysis. *Chemistry – A European Journal*, **15**, 3920–3935.
- Di Cosimo, J.I., Diez, V.K., Xu, M., Iglesia, E., and Apesteguia, C.R. (1998) Structure and surface and catalytic properties of Mg-Al basic oxides. *Journal of Catalysis*, **178**, 499–510.
- Fishel, C.T. and Davis, R.J. (1994a) Characterization of Mg-Al mixed oxides by temperature-programmed reaction of 2-propanol. *Langmuir*, **10**, 159–165.
- Fishel, C.T. and Davis, R.J. (1994b) Use of catalytic reactions to probe Mg-Al mixed-oxide surfaces. *Catalysis Letters*, **25**, 87–95.
- Gardner, E., Huntoon, K.M., and Pinnavaia, T.J. (2001) Direct synthesis of alkoxide-intercalated derivatives of hydrotalcite-like layered double hydroxides: Precursors for the formation of colloidal layered double hydroxide suspensions and transparent thin films. *Advanced Materials*, **13**, 1263–1266.
- Gordiyenko, O.I., Linnik, T.P., and Gordiyenko, E.O. (2004) Erythrocyte membrane permeability for a series of diols. *Bioelectrochemistry*, **62**, 115–118.
- Greenwell, H.C., Stackhouse, S., Coveney, P.V., and Jones, W. (2003) A density functional theory study of catalytic transesterification by tert-butoxide MgAl anionic clays. *Journal of Physical Chemistry B*, **107**, 3476–3485.
- Guimaraes, J.L., Marangoni, R., Ramos, L.P., and Wypych, F. (2000) Covalent grafting of ethylene glycol into the Zn-Al-CO₃ layered double hydroxide. *Journal of Colloid and Interface Science*, **227**, 445–451.
- Hansen, H.C.B. and Taylor, R.M. (1991) The use of glycerol intercalates in the exchange of CO₃²⁻ with SO₄²⁻, NO₃⁻ or Cl⁻ in pyroaurite-type compounds. *Clay Minerals*, **26**, 311–327.
- Kloppogge, J.T. and Frost, R.L. (1999) Fourier transform infrared and Raman spectroscopic study of the local structure of Mg-, Ni-, and Co-hydrotalcites. *Journal of Solid State Chemistry*, **146**, 506–515.
- McKenzie, A.L., Fishel, C.T., and Davis, R.J. (1992) Investigation of the surface-structure and basic properties of calcined hydrotalcites. *Journal of Catalysis*, **138**, 547–561.
- Mendelovici, E., Frost, R.L., and Kloppogge, T. (2000) Cryogenic Raman spectroscopy of glycerol. *Journal of Raman Spectroscopy*, **31**, 1121–1126.
- Meyn, M., Beneke, K., and Lagaly, G. (1990) Anion-exchange reactions of layered double hydroxides. *Inorganic Chemistry*, **29**, 5201–5207.
- Perez-Ramirez, J., Abello, S., and van der Pers, N.M. (2007) Memory effect of activated Mg-Al hydrotalcite: in situ XRD studies during decomposition and gas-phase reconstruction. *Chemistry – A European Journal*, **13**, 870–878.
- Rao, K.K., Gravelle, M., Valente, J.S., and Figueras, F. (1998) Activation of Mg-Al hydrotalcite catalysts for aldol condensation reactions. *Journal of Catalysis*, **173**, 115–121.
- Reichle, W.T. (1985) Catalytic reactions by thermally activated, synthetic, anionic clay-minerals. *Journal of Catalysis*, **94**, 547–557.
- Remias, R., Kukovec, A., Daranyi, M., Kozma, G., Varga, S., Konya, Z., and Kiricsi, I. (2009) Synthesis of zinc glycerolate microstacks from a ZnO nanorod sacrificial template. *European Journal of Inorganic Chemistry*, 3622–3627.
- Rey, F. and Fornes, V. (1992) Thermal decomposition of hydrotalcites – an infrared and nuclear magnetic resonance spectroscopic study. *Journal of the Chemical Society – Faraday Transactions*, **88**, 2233–2238.
- Sels, B.F., De Vos, D.E., and Jacobs, P.A. (2001) Hydrotalcite-like anionic clays in catalytic organic reactions. *Catalysis Reviews – Science and Engineering*, **43**, 443–488.
- Stanimirova, T. and Hibino, T. (2006) Ethylene glycol intercalation in MgAlCO₃ hydrotalcite and its low-temperature intermediate phases. *Applied Clay Science*, **31**, 65–75.
- Tichit, D., Lhouty, M.H., Guida, A., Chiche, B.H., Figueras, F., Auroux, A., Bartalini, D., and Garrone, E. (1995) Textual properties and catalytic activity of hydrotalcites. *Journal of Catalysis*, **151**, 50–59.
- Tichit, D., Bennani, M.N., Figueras, F., and Ruiz, J.R. (1998) Decomposition processes and characterization of the surface

- basicity of Cl^- and CO_3^{2-} hydrotalcites. *Langmuir*, **14**, 2086–2091.
- Tichit, D., Bennani, M.N., Figueras, F., Tessier, R., and Kervennal, J. (1998) Aldol condensation of acetone over layered double hydroxides of the meixnerite type. *Applied Clay Science*, **13**, 401–415.
- van Bokhoven, J.A., Roelofs, J.C.A.A., de Jong, K.P., and Koningsberger, D.C. (2001) Unique structural properties of the Mg-Al hydrotalcite solid base catalyst: An in situ study using Mg and Al K-edge XAFS during calcination and rehydration. *Chemistry – A European Journal*, **7**, 1258–1265.
- Williams, G.R. and O'Hare, D. (2006) Towards understanding, control and application of layered double hydroxide chemistry. *Journal of Materials Chemistry*, **16**, 3065–3074.
- Winter, F., Xia, X.Y., Hereijers, B.P.C., Bitter, J.H., van Dillen, A.J., Muhler, M., and de Jong, K.P. (2006) On the nature and accessibility of the Bronsted-base sites in activated hydrotalcite catalysts. *Journal of Physical Chemistry B*, **110**, 9211–9218.
- Wypych, F., Schreiner, W.H., and Marangoni, R. (2002) Covalent grafting of ethylene glycol and glycerol into brucite. *Journal of Colloid and Interface Science*, **253**, 180–184.
- Xi, Y. and Davis, R.J. (2008) Influence of water on the activity and stability of activated Mg-Al hydrotalcites for the transesterification of tributyrin with methanol. *Journal of Catalysis*, **254**, 190–197.
- Xi, Y. and Davis, R.J. (2009) Influence of textural properties and trace water on the reactivity and deactivation of reconstructed layered hydroxide catalysts for transesterification of tributyrin with methanol. *Journal of Catalysis*, **268**, 307–317.
- Xi, Y. and Davis, R.J. (2010) Intercalation of ethylene glycol into yttrium hydroxide layered materials. *Inorganic Chemistry*, **49**, 3888–3895.
- Yang, W.S., Kim, Y., Liu, P.K.T., Sahimi, M., and Tsotsis, T.T. (2002) A study by in situ techniques of the thermal evolution of the structure of a Mg-Al- CO_3 layered double hydroxide. *Chemical Engineering Science*, **57**, 2945–2953.
- Zelent, B., Nucci, N.V., and Vanderkooi, J.M. (2004) Liquid and ice water and glycerol/water glasses compared by infrared spectroscopy from 295 to 12 K. *Journal of Physical Chemistry A*, **108**, 11141–11150.

(Received 22 January 2010; revised 27 May 2010; Ms. 402; A.E. F. Bergaya)